

Novel Supramolecular Systems Based on β -Cyclodextrin: Synthesis, Characterization, and Applications as Drug Carriers for Streptomycin

Kamal M. Dawood ^{1,*} , Hemat M. Dardeer ², Marwa El-Sayed ³, Lamiaa Mageed ⁴, Hany A. Abdel atty ⁵, Mohamad A. Raslan ^{5,6}, Shaaban K Mohamed ⁷, Omar A. Farghaly ⁸, Ayman Nafady ^{9,*}

¹ Chemistry Department, Faculty of Science, Cairo University, Giza 12613, Egypt

² Chemistry Department, Faculty of Science, South Valley University, Qena 83523, Egypt

³ Department of Medical Microbiology and Immunology, Faculty of Medicine, South Valley University, Qena 83523, Egypt

⁴ Biochemistry Department, National Research Centre, Dokki 12622, Egypt

⁵ Chemistry Department, Faculty of Science, Aswan University, Aswan, Egypt

⁶ Faculty of Technological Industry and Energy, Thebes Technological University, Thebes, Luxor 85863, Egypt

⁷ Chemistry and Environmental Division, Manchester Metropolitan University, Manchester, UK

⁸ Biochemistry Department, Faculty of Pharmacy, Al-Azhar University, Assiut, Egypt

⁹ Department of Chemistry, College of Science, King Saud University, Riyadh 11451, Saudi Arabia

* Correspondence: kmdawood@sci.cu.edu.eg (K.M.D);

Received: 27.04.2024; Accepted: 8.01.2025; Published: 20.12.2025

Abstract: Recently, polyrotaxanes containing cyclodextrin have been utilized in different fields, particularly in pharmaceutical applications. Herein, we describe a facile approach to enhance the efficiency and biological activity of the Streptomycin antibiotic by incorporating it into two novel pseudopolyrotaxanes, Chs/ β -CD (1) and PSSNa/ β -CD (2), as promising carriers. The chemical composition of the designed materials and Streptomycin (D) was confirmed before and after loading into pseudopolyrotaxanes (1 and 2) using FT-IR and ¹H-NMR spectroscopy. The surface morphologies of the obtained carriers and drug were probed by scanning electron microscopy (SEM), whereas the crystallinity of the final products was evidenced by XRD. The thermal gravimetric analysis (TGA) of the prepared pseudopolyrotaxanes and the thermal stability of Streptomycin (D) before and after loading onto the pseudopolyrotaxanes were examined. Importantly, the antimicrobial activity of Streptomycin was examined versus some Gram-negative and Gram-positive bacteria (*E. coli* and *S. aureus*) before and after loading onto the polymers. The MIC values of the tested compounds Chs/ β -CD (1), PSSNa/ β -CD (2), Chs/ β -CD/D (3), and PSSNa/ β -CD/D (4) against *S. aureus* and *E. coli* ranged from 16 ~ 0.125 μ g/mL. The drug, after loading onto Chs/ β -CD, has inhibited bacterial growth, with an MIC of 4 μ g/mL compared with Streptomycin (16 μ g/mL). The major outcome of this study attests that loading of Streptomycin onto the newly designed pseudopolyrotaxanes drastically enhanced its physicochemical and biochemical properties, thereby affecting its pharmacological applications.

Keywords: β -cyclodextrin; biopolymers; Streptomycin; drug delivery; TGA, antibiotic.

© 2025 by the authors. This article is an open-access article distributed under the terms and conditions of the Creative Commons Attribution (CC BY) license (<https://creativecommons.org/licenses/by/4.0/>), which permits unrestricted use, distribution, and reproduction in any medium, provided the original work is properly cited. The authors retain copyright of their work, and no permission is required from the authors or the publisher to reuse or distribute this article, as long as proper attribution is given to the original source.

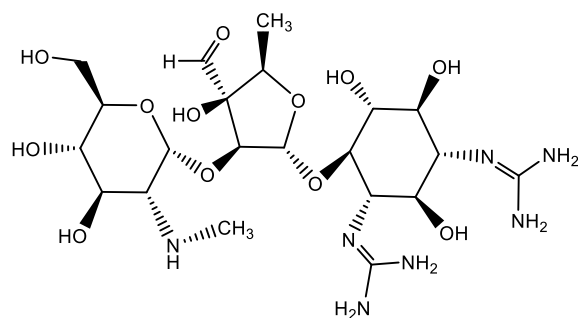
1. Introduction

A drug designer has always focused on finding a compound that can be used to improve the properties of a known drug or discover a new type of drug. Cyclodextrins (CDs), for example, have an essential role in daily life as invisible constituents of common food products,

cosmetic and toiletry goods, textiles, and as enabling excipients in various medicinal products [1-4]. Consequently, the future without cyclodextrins is hard to envision. The enzymatic breakdown of starch produces cyclic oligosaccharides, or CDs, which have a special truncated cone form with a hydrophilic outer rim and a hydrophobic inner ring. The less polar guest molecules may fully or partially insert into the CDs' cavities [5]. One of the most common types of CDs is β -cyclodextrin (β -CD), which has seven glucose units and is inexpensive and easy to synthesize [6,7]. β -CD can form inclusion complexes with a variety of drugs via hydrophobic, electrostatic, and Van der Waals interactions, as well as hydrogen bonding [8-11]. CD polymers could improve the physicochemical and biopharmaceutical properties of drugs by forming inclusion complexes with drugs in solution, masking organoleptic properties, enhancing permeability, and improving solubility. In addition, CDs reduce volatility and toxic effects [12,13]. Polymers have significant uses in drug formulations and delivery devices due to their high surface area and bulk properties. They are acting as drug carriers. As a result, they ought to be soluble, nontoxic, and exhibit enormous development as hydrogels and liposomes. In their basic form, they function passively to extend circulation time and slow down the drug breakdown. The safe excretion of the drug is a vital issue as well [14].

Numerous organic polymers, synthetic polymers, and copolymers are investigated as drug delivery carriers [15], and as solid support catalysts for organic synthesis [16-18]. Gelatin, albumin, chitosan, and hyaluronic acid are among the most popular natural polymers. The most widely used synthetic polymers are polyethylene glycol (PEG), polylactic acid (PLA), polyvinyl alcohol (PVA), and polyacrylic acid derivatives. The most widely used copolymer across a variety of pharmaceutical products is polylactic-co-glycolic acid (PLGA). These copolymers, composed of many subunits from two or more unique monomers, offer greater flexibility for various therapeutic purposes [19-21]. Chitosan is a naturally occurring polymer that has been extensively studied as a linear amino polysaccharide. Chitin from different animal sources was partially deacetylated to produce chitosan. It is a cationic copolymer made of β -1,4 of D-glucosamine and N-acetylglucosamine. Due to its biocompatible, biodegradable, mucoadhesive, antimicrobial, and nontoxic characteristics, chitosan is used as a good chelating agent for metal ions, a coating and gelling agent, and a drug delivery carrier for numerous small- and macromolecules [15]. Cyclodextrin pseudopolyrotaxanes have attractive supramolecular structures with unique properties, designed by threading a polymer chain or a long molecule through many CD rings. Numerous synthetic polymers, such as biopolymers, conducting polymers, dyes, polypeptides, and enzymes, can form inclusion complexes with CDs to prepare pseudopolyrotaxanes. These types of supramolecular structures are extremely useful in diverse application areas [22-28].

An antibiotic is a specific type of antimicrobial agent that works against bacteria. It is the most crucial form of antibacterial agent for preventing and treating bacterial infections [29,30]. They could either eliminate or suppress bacterial growth [31]. Antibiotics are ineffective against viruses such as influenza or the common cold; antiviral drugs, on the other hand, are used to inhibit viruses [32]. In contrast to antibiotics, which are a significant class of antibacterials used more frequently in medicine, antibacterials include antiseptic medications, antibacterial soaps, and chemical disinfectants [33], and are occasionally used in animal feed. A number of bacterial illnesses, including endocarditis, tuberculosis, brucellosis, Burkholderia infection, plague, tularemia, and rat bite fever, are treated with the antibiotic Streptomycin (Scheme 1). It is frequently administered along with isoniazid, rifampicin, and pyrazinamide for active tuberculosis, and is given by injection into a muscle or vein [34].



Streptomycin (D)

Scheme 1. Chemical structure of the antibiotic used (**D**).

Vertigo, nausea, facial numbness, fever, and rash are typical side effects of Streptomycin. The use of Streptomycin throughout pregnancy has the potential to leave the unborn child permanently deaf. It appears safe to use during lactation. It is not advised for those with myasthenia gravis or other neuromuscular diseases. It is an aminoglycoside [35, 36] and acts by avoiding the production of proteins by 30S ribosomal subunits. Streptomycin causes misreading of the mRNA, leading to the incorporation of incorrect amino acids into the growing polypeptide chain and the production of nonfunctional or defective proteins, thereby inhibiting bacterial growth. Streptomycin primarily targets bacterial ribosomes and does not affect human ribosomes to the same extent. From this point, the present study focuses on the synthesis and design of a new type of pseudopolyrotaxane structure that could enhance the physicochemical and biopharmaceutical properties of Streptomycin. Thus, two new inclusion polymer complexes containing cyclodextrin, chitosan, polystyrene sulphonate, Chs/ β -CD (1) and PSSNa/ β -CD (2) are synthesized as antibacterial systems. They also served as carriers for Streptomycin as Chs/ β -CD/D (3) and PSSNa/ β -CD/D (4). The current findings revealed that the drug's physicochemical properties also improve its antibacterial efficacy.

2. Materials and Methods

2.1. Materials.

Streptomycin, β -cyclodextrin, chitosan with a deacetylation degree above 85%, and dimethylformamide (DMF) were purchased from Merck Co., Germany. Poly(styrene sulfonic acid) sodium salt and glacial acetic acid were obtained from Alfa Aesar GmbH and Co. KG. The thermal stability of the prepared materials was investigated using TGA (SDT Q600 V20.9 Build 20) with an argon flow rate of 40 mL/min and a heating rate of 15°C/min to 300°C. The thermal analyzer was equipped with a data acquisition and handling system (TA-50WSI).

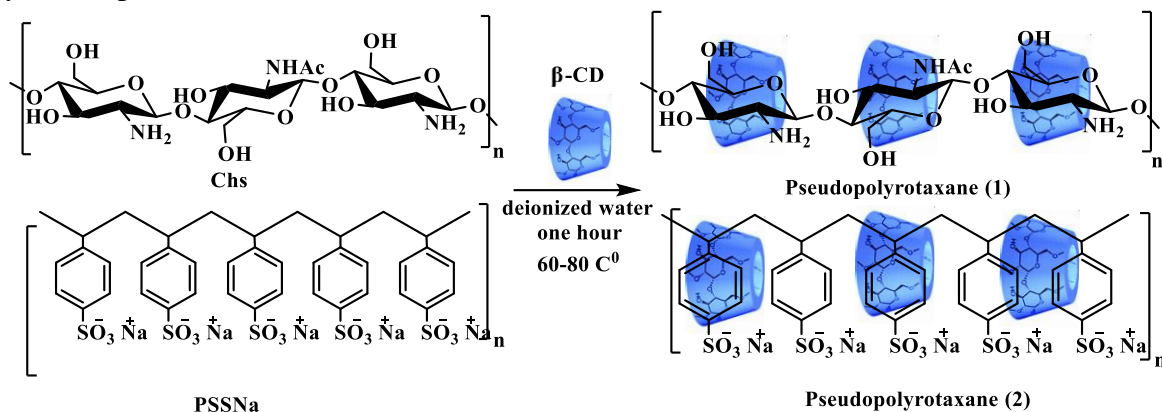
2.2. Synthesis of the new carriers' polymers.

2.2.1. Synthesis of pseudopolyrotaxane Chs/ β -CD (1).

The preparation of the Chitosan solution was done via dissolving 1 g of chitosan in 50 ml of (1% v/v) glacial acetic acid for 2 h at 60°C in a magnetic stirrer until a clear solution was obtained, then the β -cyclodextrin solution was also prepared by dissolving 1.5 g of β -CD in 50 ml of deionized water for 1 h at 60°C. The two solutions were mixed and stirred for an additional 24 h at 60°C. The obtained hydrogel was poured into a petri dish, and solvent evaporation at room temperature yielded the inclusion polymer complex (1) as a pale brown powder (85% yield, m.p. >300°C), as shown in Scheme 2.

2.2.2. Synthesis of pseudopolyrotaxane PSSNa/ β -CD (2).

According to Scheme 2, poly(styrene sulfonic acid) sodium salt (PSSNa) solution was prepared by dissolving 1 g of PSSNa in 50 ml of deionized water for 1 h at 60°C in a magnetic stirrer, then β -cyclodextrin solution was prepared by dissolving 1.5 g of β -CD in 50 ml of deionized water and mixed for 1 h at 80°C. The mixed solution was agitated for 24 h. at 60°C. The hydrogel was produced, then poured into a petri dish, and, at room temperature, the solvent was evaporated, yielding the inclusion polymer complex (2) as a pale-yellow powder (90% yield, m.p. >300°C).



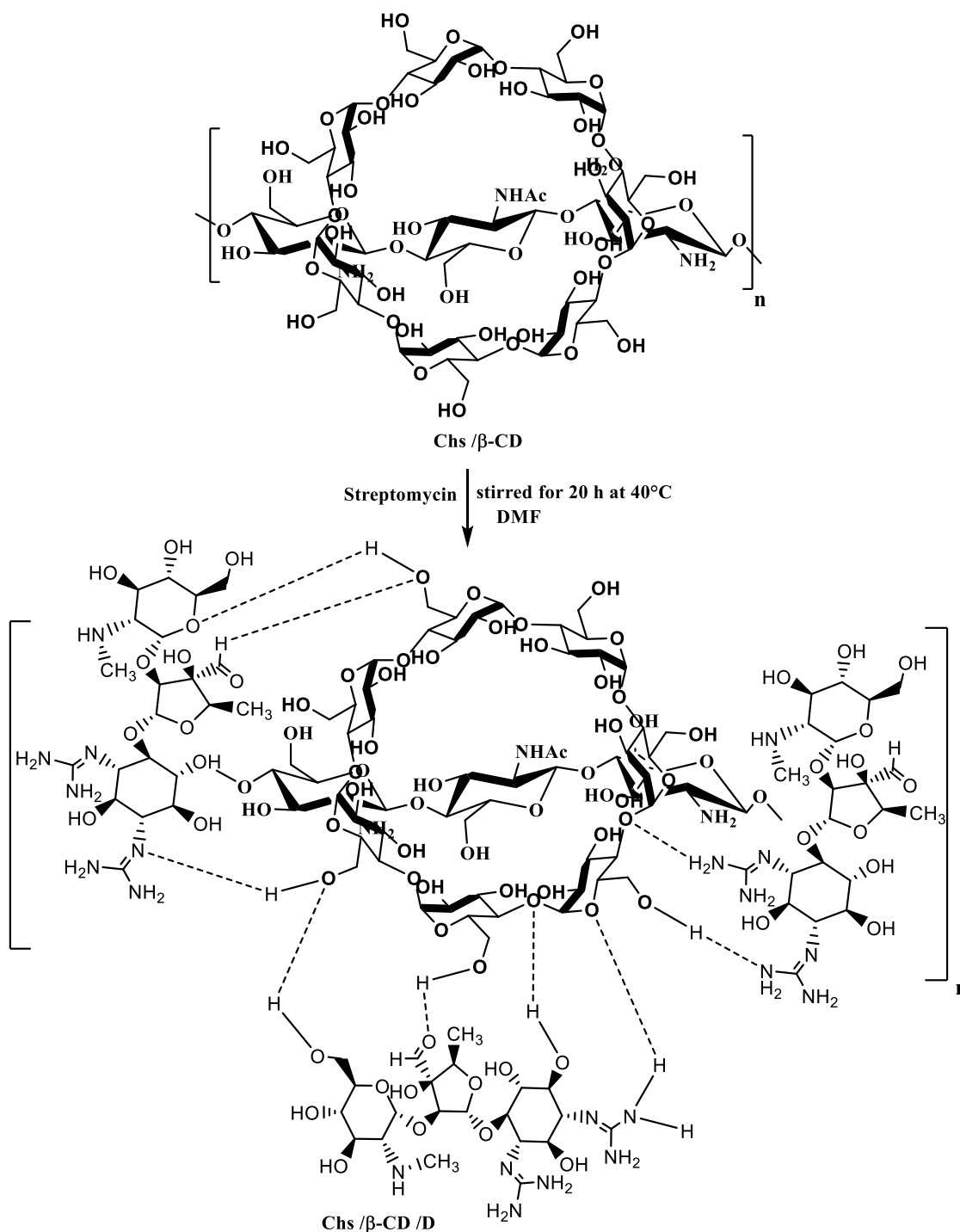
Scheme 2. Synthetic route for the pseudopolyrotaxane (1) Chs/ β -CD; (2) PSSNa/ β -CD.

2.2.3. Loading Streptomycin (D) on pseudopolyrotaxanes Chs/ β -CD (1) and PSSNa/ β -CD (2) to form Chs/ β -CD/D (3) PSSNa/ β -CD/D (4).

Streptomycin (D) was loaded onto the pseudopolyrotaxanes (1 and 2) via a colloidal tectonic structural approach, then 0.5 g of the inclusion complex was dissolved in 30 mL of DMF to produce a stable hydrogel. At room temperature, 0.25 g of the drug was dissolved in 10 ml of DMF and added to the mixture. The reaction mixture was stirred for 20 h at 40°C. The obtained hydrogel emulsion was dried by freeze-drying to yield brown and yellow crystals, Chs/ β -CD/D (3) and PSSNa/ β -CD/D (4), as shown in Schemes 3 and 4. There are no side effects from DMF, which is used as a solvent in the loading process, as a small amount is used and no chemical reaction occurs between DMF and the materials. Samples are also dried before being applied to the bacteria.

2.2.4. Antibacterial test.

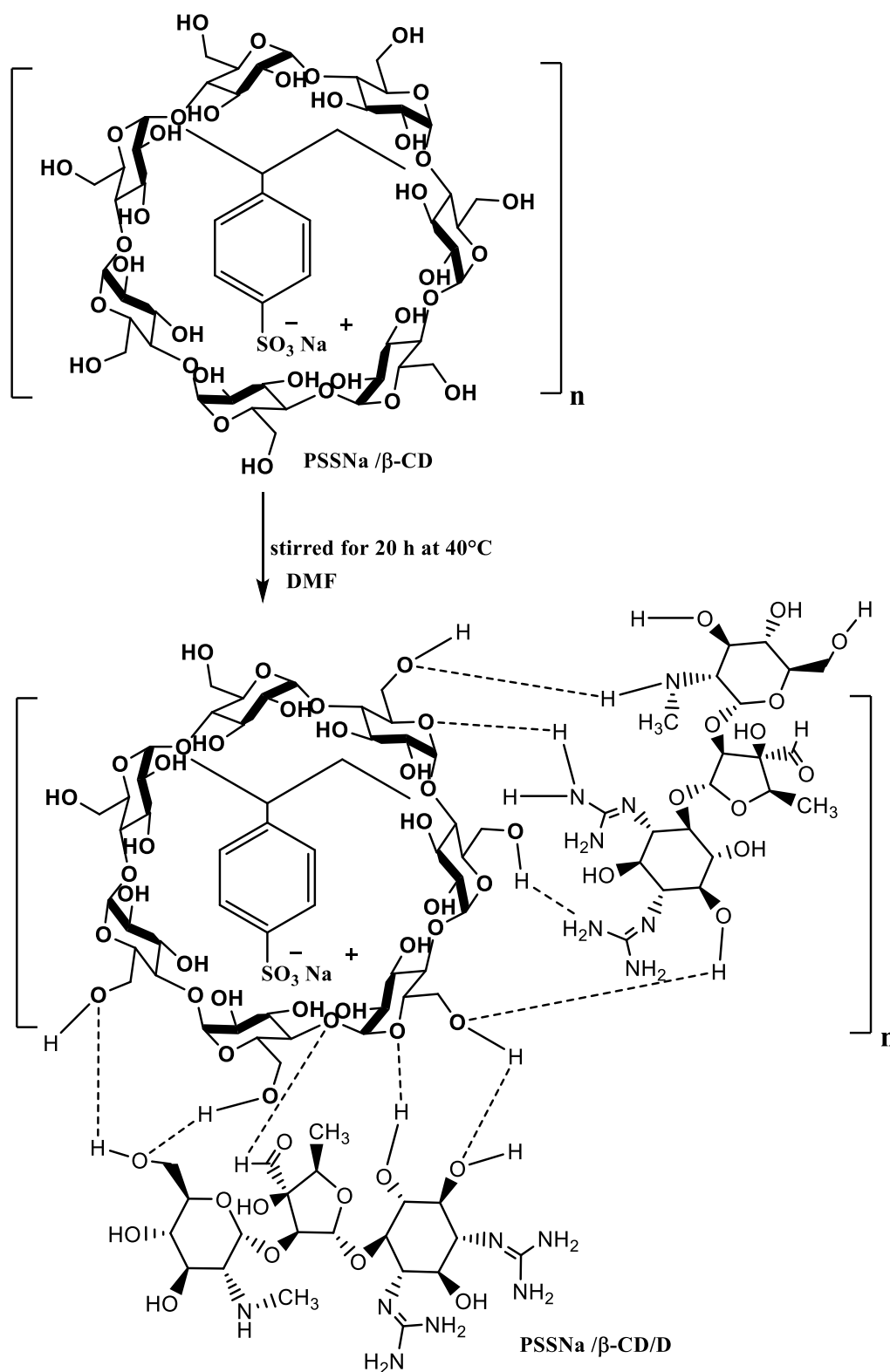
After overnight liquid cultures of *Staphylococcus aureus* (NCTC 8325-4) and *Escherichia coli* (BAA-2471), the antibacterial activity of drug (D), Chs/ β -CD (1), PSSNa/ β -CD (2), Chs/ β -CD/D (3), and PSSNa/ β -CD/D (4) was quantified by measuring the MIC (Minimal Inhibitory Concentration), which is the minimum concentration needed from the antimicrobial agent to prevent the growth of microorganisms, a bacterial solution with (105 CFU/mL) in 100 L MHB (Mueller-Hinton broth) was added to a microtitre plate (Nucleon, Germany) with two-fold dilutions of an antimicrobial agent, and the plate was then incubated at 37°C, to assess whether the broth was adequate for promoting the growth of the organism and verify its sterility. The outcomes included information from three distinct experiments.



Scheme 3. Synthetic route for loading of Streptomycin (D) on pseudopolyrotaxane Chs/β-CD.

2.2.5. The effect of target compounds on biofilm formation.

At a final concentration of 5×10^5 bacteria per mL, overnight cultures of *S. aureus* NCTC 8325-4 were diluted, then added to a new BHI in a 96-well microplate. The compound solution (16 μg/mL) was added to the wells, whereas PBS alone was added to the polymer-free wells as controls. After incubating the biofilms for 24 hours at 37°C with gentle shaking (35 rpm), the wells were rinsed with PBS and stained for 20 minutes with 0.1% (w/v) crystal violet. After properly washing the plate with water, 200 L of 95% ethanol was added for 20 minutes to remove the biofilm bacteria stain. Using a plate reader, the alcohol solution's absorbance was measured at 595 nm.



Scheme 4. Synthetic route for loading of Streptomycin (**D**) on pseudopolyrotaxane PSSNa/β-CD.

2.3. Characterizations.

2.3.1. Fourier-transform infrared (FTIR).

The structure of the obtained pseudopolyrotaxanes and the Streptomycin before and after loading was studied using Fourier-transform infrared spectroscopy at room temperature using an infrared spectrometer (Jasco Model 4100 – Japan) in the wavenumber region of 4000–400 cm⁻¹.

2.3.2. ¹H-NMR spectroscopy.

The chemical structure of the synthesized inclusion polymer complex (1,2). Also, Streptomycin after loading onto the prepared carriers was confirmed by ¹H NMR, recorded at 25°C on a Bruker AM-400 NMR spectrometer (Germany) at 400 MHz. The synthesized materials were dissolved in Aldrich DMSO-d₆ solution.

2.3.3. X-ray diffraction (XRD).

The phase structure and crystallite size of the products were investigated by XRD measurements taken at room temperature with a powder diffractometer (Bruker D8 Advance, Germany) equipped with a Cu K α radiation source, $\lambda = 1.5406 \text{ \AA}$ and 2θ in the range (5–80°).

2.3.4. Scanning electron microscope (SEM).

To examine the phase structure and crystallite size of the samples, X-ray diffraction spectra were recorded at room temperature using a powder diffractometer (Bruker D8 Advance, Germany) with a Cu K α radiation source ($\lambda = 1.5406 \text{ \AA}$) and 2θ in the range of 5–80°. A scanning electron microscope (SEM) (JEOL SEM Model JSM-5500 - Japan) was utilized to recognize the morphology of the materials obtained at an accelerating voltage of 10 kV.

2.3.5. Thermogravimetric analysis (TGA).

The thermal stability of the drug after loading on the prepared carriers was measured using a TGA (SDT Q600 V20.9 Build 20) with a 5°C/min heating rate up to 800°C and a 5 ml/min nitrogen gas flow. A data collection and handling mechanism is built into the thermal analyzer (TA-50WSI).

3. Results and Discussion

3.1. FT-IR studies.

Scheme 2 outlines the proposed mechanism for the synthesis of the pseudopolyrotaxanes Chs/ β -CD (1) and PSSNa/ β -CD (2). The polymer chains (Chs or PSSNa) were inserted into the macrocyclic molecules of β -CD via a threading method, in which chitosan chains and/or polystyrene sulfonate were threaded through the β -CD rings to form inclusion polymer complexes [36,37]. The effective forces on forming these complexes are hydrogen bonding, Vanderwalls forces, electrostatic bonds, and hydrophobic-hydrophobic interactions. Scheme 3 shows the proposed mechanism for loading Streptomycin into Chs/ β -CD (1). Thus, Streptomycin was loaded onto the Chs/ β -CD (1) by the formation of strong hydrogen bonding between the functional groups in the Chs/ β -CD (NH₂, NH, OH) inclusion complex and the active groups in Streptomycin (NH₂, NH, CHO). The formation of a large number of hydrogen bonds improves the loading process and the stability of the drug [2].

Scheme 4 shows the loading process of Streptomycin on PSSNa/ β -CD (2), in which Streptomycin was loaded by the formation of hydrogen bonding between (NH₂, NH, -O-, CHO) groups in Streptomycin and the active groups present in the inclusion polymer complex (PSSNa/ β -CD). The chemical structure of pseudopolyrotaxane (1) was established by FT-IR spectra that showed some characteristic bands as follows: at 3382 cm⁻¹ for hydroxyl groups

and at 2926 cm^{-1} , a characteristic band for CH aliphatic in addition to a band at 1159 cm^{-1} due to C-O-C groups and a band at 1030 cm^{-1} due to C-H vibrations. The absorption bands of symmetric $\nu[\text{OH}]$ stretching and $\nu[\text{CH-aliphatic}]$ were shifted to lower frequencies compared to those of pure $\beta\text{-CD}$ (Figure 1 due to the formation of strong hydrogen bonds. Also, the absorption bands of $\nu[\text{O-H}]$ stretching and $\nu[\text{CH-aliphatic}]$ were transported into lower frequencies as compared to those of pure $\beta\text{-CD}$. Moreover, the absorption bands of $\nu[\text{C-O-C}]$ and $\nu[\text{C-O}]$ stretching were shifted to higher frequencies. Table 1 displays the variation in absorption bands between pure $\beta\text{-CD}$ and Chs/ $\beta\text{-CD}$ (1). The change in absorption band may clearly indicate the evolution of the inclusion complex between the chitosan and $\beta\text{-CD}$ macrocycles. The rise in frequency is owing to the insertion of chitosan chains through the electron-rich cavities of the $\beta\text{-CD}$ ring. In contrast, the decline in frequency results from the formation of Vander Waals forces and H-bonds between the hydroxyl groups of $\beta\text{-CD}$ and the hydroxyl and amino groups of chitosan. The FT-IR spectrum of Streptomycin exhibited a band at 3370 cm^{-1} correlated to the NH_2 groups, and a band at 2930 cm^{-1} due to the CH-aliphatic group. The absorption band at 1145 cm^{-1} , which is referred to as the C-O-C vibration group, and the band at 1031 cm^{-1} due to C-O groups (Figure 1. The changes in absorbance bands between pure drug and Chs/ $\beta\text{-CD/D}$ (3) are summarized in Table 1. The change of the Streptomycin intensity before and after loading onto Chs/ $\beta\text{-CD}$ (1) is owing to the forces of Vander Waals and H-bonds between OH and NH_2 groups, also, O and N atoms of pure drug and (OH, NH, and NH_2) groups of Chs/ $\beta\text{-CD}$ (1).

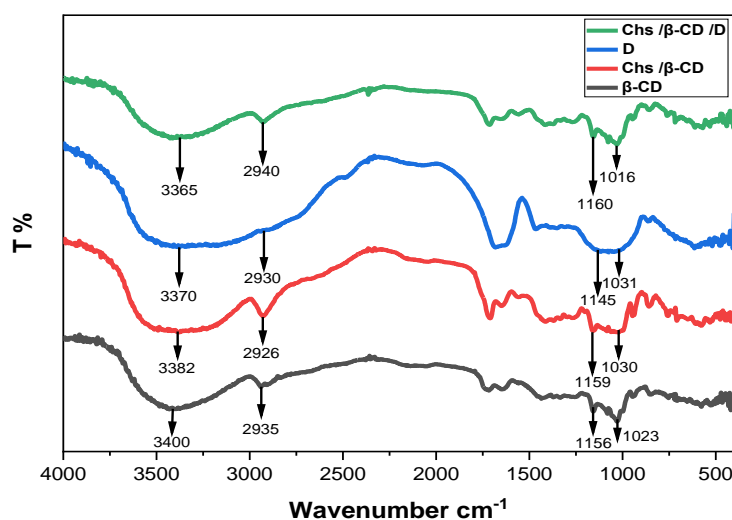


Figure 1. FT-IR spectra of pure $\beta\text{-CD}$, pure Drug, Chs/ $\beta\text{-CD}$ (1), and Chs/ $\beta\text{-CD/D}$ (3).

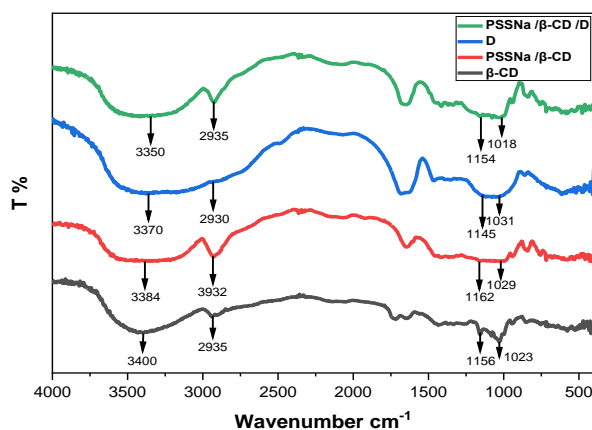


Figure 2. FT-IR spectra of pure $\beta\text{-CD}$, pure Drug, PSSNa/ $\beta\text{-CD}$ (2), and PSSNa/ $\beta\text{-CD/D}$ (4).

Table 1. The difference in the frequencies between β -CD, Chs/ β -CD (1), and between pure Drug and Chs/ β -CD/D (3).

Functional group	Wavenumber, cm^{-1}		$\Delta\delta$	Wavenumber, cm^{-1}		$\Delta\delta$
	β -CD	Chs/ β -CD		D	Chs/ β -CD/D	
ν [O-H]- ν [NH ₂] stretching	3400	3382	-18	3370	3365	-5
ν [CH-aliphatic]	2935	2926	-9	2930	2940	+10
ν [C-O-C] vibration	1156	1159	+3	1145	1160	+15
ν [C-O] stretching	1023	1030	+7	1031	1016	-15

Pseudopolyrotaxane PSSNa/ β -CD (2) is described in Scheme 2, and the frequency of the examined functional groups via FT-IR spectroscopy displayed many characteristic bands, for example, at 3384 cm^{-1} concerning hydroxyl groups, a band at 3012 cm^{-1} belongs to CH aromatic, a characteristic band at 1141 cm^{-1} due to C-O-C vibration, and a band at 1029 cm^{-1} due to C-O groups. The absorption band of ν [OH] symmetric stretching and ν [CH-aromatic] was transferred to a lower frequency in contrast to those in pure β -CD (Figure 2). Also, the absorption band for both ν [O-H] stretching and ν [CH-aromatic] was moved to a lower frequency when compared to those in pure β -CD. Furthermore, the absorption bands of the ν [C-O-C] vibration and the ν [C-O] stretching were shifted to higher frequencies [2]. Table 2 outlines the absorbance bands' alterations for pure β -CD and PSSNa/ β -CD (2). The movement of the absorbance bands may result from the formation of an inclusion complex between poly(styrene sulfonic acid) sodium salt and β -CD. Because of the addition of the poly(styrene sulfonic acid) sodium salt chain through the inner cavity of the cyclodextrin rings, the frequency was increased. Otherwise, the reduction in frequency is attributable to van der Waals forces and H-bonds between β -CD and poly(styrene sulfonic acid) sodium salt groups [36]. The variances of absorbance bands between pure drug and pseudopolyrotaxane/drug (4) are presented in Table 2. The alteration in the strength of Streptomycin before and after loading onto PSSNa/ β -CD (2) was owing to Vander Waals forces and H-bonds of the active groups in pure drug and the characteristic groups in the PSSNa/ β -CD (2) and gave a good indication for the loading of the drug into PSSNa/ β -CD (2)

Table 2. The difference in the frequencies between β -CD and PSSNa/ β -CD and between pure Drug and PSSNa/ β -CD/D (4).

Functional group	Wavenumber, cm^{-1}		$\Delta\delta$	Wavenumber, cm^{-1}		$\Delta\delta$
	β -CD	PSSNa/ β -CD		D	PSSNa/ β -CD/D	
ν [O-H]- ν [NH ₂] stretching	3400	3384	-16	3370	3350	-20
ν [CH-aliphatic]- ν [CH-aromatic]	2935	2932	-3	3012	3006	-6
ν [C-O-C] vibration	1156	1141	+15	1145	1154	+9
ν [C-O] stretching	1023	1029	+6	1031	1018	-13

3.2. ¹H NMR analysis.

The chemical structure of Chs/ β -CD (1) was confirmed by ¹H NMR spectroscopy. ¹H NMR spectrum of Chs/ β -CD (1) showed the appearance of signals due to aliphatic protons of β -CD in addition to the aliphatic protons of chitosan in the range of δ 3.18-4.78 ppm and a signal due to secondary alcohol protons at δ 5.73 ppm (Figure 3). Furthermore, the appearance of peaks due to (NH-CO-) groups in the region δ 8.08-8.17 ppm. The ¹H NMR spectrum of the PSSNa/ β -CD (2). Figure 3 indicated signals due to the aliphatic polystyrene chain at δ 1.08

(CH₂) and 1.87 (CH), and β-CD protons appeared at δ 3.30-5.78 ppm. The chemical structure of the drug after loading into Chs/β-CD (1) is shown in Figure 3.

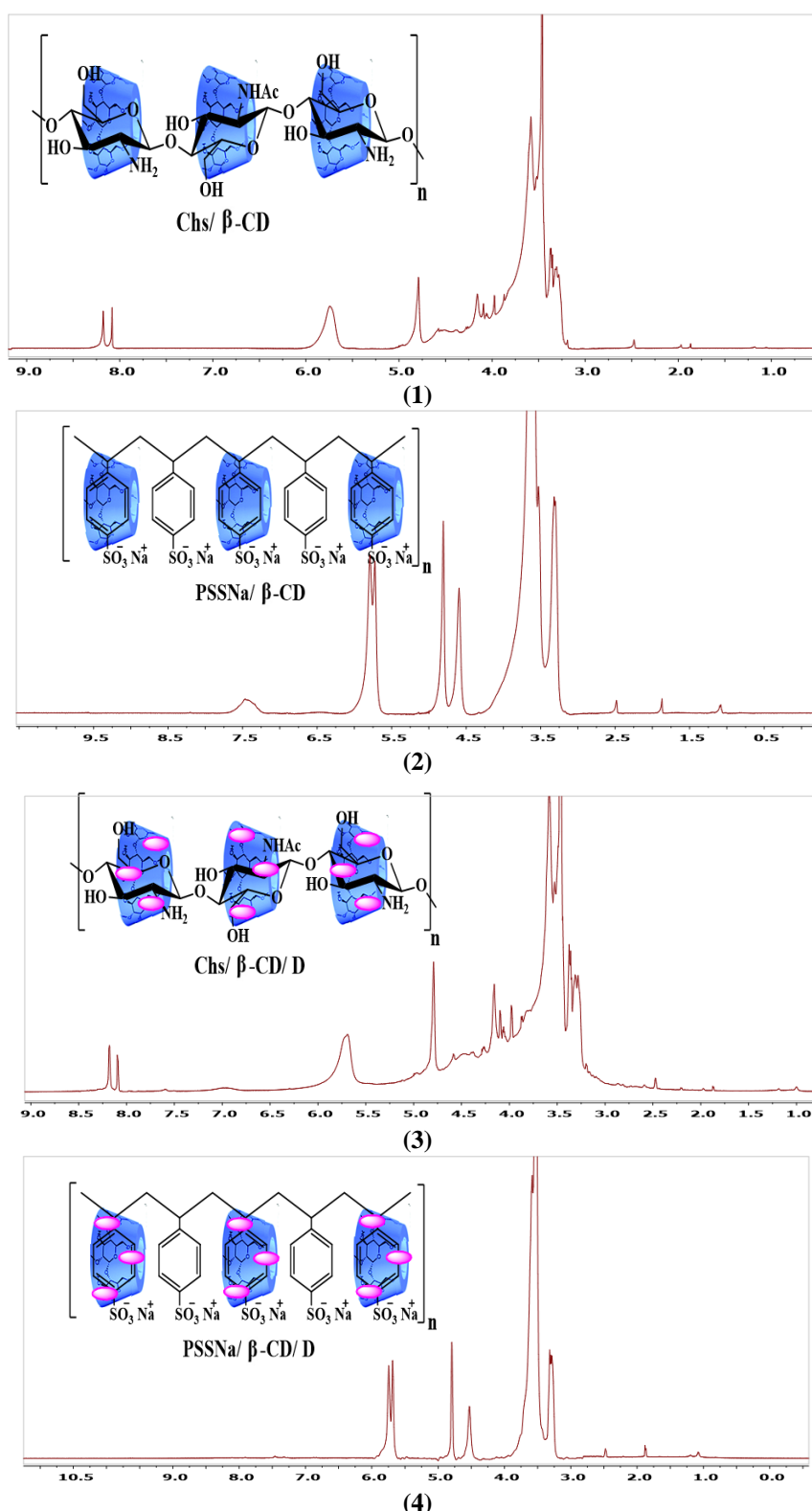


Figure 3. ¹H NMR for (1) Chs/β-CD; (2) PSSNa/β-CD; (3) Chs/β-CD/D; (4) PSSNa/β-CD/D in DMSO-d₆.

The ¹H-NMR spectra of Chs/β-CD/D (3) indicate the appearance of a characteristic peak due to two methyl groups (CH₃ and NHCH₃) of Streptomycin (D) at δ 2.22 and 2.49 ppm. In addition, the presence of signals due to the aliphatic protons of β-CD and chitosan is observed in the region δ 3.19-5.69 ppm. As shown in Figure 3. The ¹H NMR spectrum of

PSSNa/ β -CD/D (4) indicated the appearance of characteristic peaks due to polystyrene chain at δ 1.08 (CH₂) and 1.86 (CH) in addition to the presence of two signals for two methyl groups (CH₃, NHCH₃) of Streptomycin (D) at δ 1.88 and 2.47 ppm, in addition to the presence of signals due to aliphatic protons of β -CD in the region δ 3.28-5.74 ppm, as well as the appearance of the aromatic protons at δ 7.56 ppm.

3.3. XRD analysis.

XRD analysis demonstrates the loading of Streptomycin (D) on the two prepared carriers, Chs/ β -CD (1) and PSSNa/ β -CD (2), by comparing the crystal size and crystallinity of Streptomycin (D) before and after loading. The phase structure and the crystallite size of Streptomycin (D), Chs/ β -CD (1), Chs/ β -CD/D (3), PSSNa/ β -CD (2), and PSSNa/ β -CD/D (4) were investigated in Figures 4,5. XRD spectra were documented in the range of 5°–80°. The characteristic diffraction peaks of Streptomycin (D), Chs/ β -CD (1), Chs/ β -CD/D (3), PSSNa/ β -CD (2), and PSSNa/ β -CD/D (4) were observed at 2 θ (Table 3). From the results, it was observed that the crystalline nature of pure streptomycin D shows sharp peaks at 2 θ = 13.68°, 16.48°, 18.14°, 20.35°, and 21.22°, with a crystallinity value of 12.2% (indicating an amorphous nature). Figure 4. On the other hand, the XRD pattern of Streptomycin after loading into the pseudopolyrotaxane Chs/ β -CD (1) exemplified a decrease in the signal intensities to 10.48°, 12.27°, 18.00°, 19.35°, and 20. Similarly, the peaks of D were shifted to 10.70°, 12.50°, 17.76°, 19.63°, and 20.86° upon loading with PSSNa/ β -CD (2). The difference in the XRD pattern is due to loading development and the formation of hydrogen bonds between the streptomycin drug and the pseudopolyrotaxanes (1, 2), Figures 4 and 5, Table 3. The crystallinity value of Streptomycin (D) after loading into pseudopolyrotaxane Chs/ β -CD (1) and pseudopolyrotaxane PSSNa/ β -CD (2) was increased to 76.8% and 64.2%, respectively.

The XRD diffractogram of the pure chitosan exhibits two prominent broad peaks at ~ 10.96° and ~ 19.50° [6]. These two peaks are characteristic topographies of the semi-crystalline nature of chitosan. In addition, these peaks are due to hydroxyl and amino groups in the chitosan polymer. For pseudopolyrotaxane Chs/ β -CD (1), these peaks display some structural changes, shifting to higher angles at ~12.27° and ~20.5°, and a clear increase in intensity with more sharpening. These new alterations give more evidence for the formation of (1).

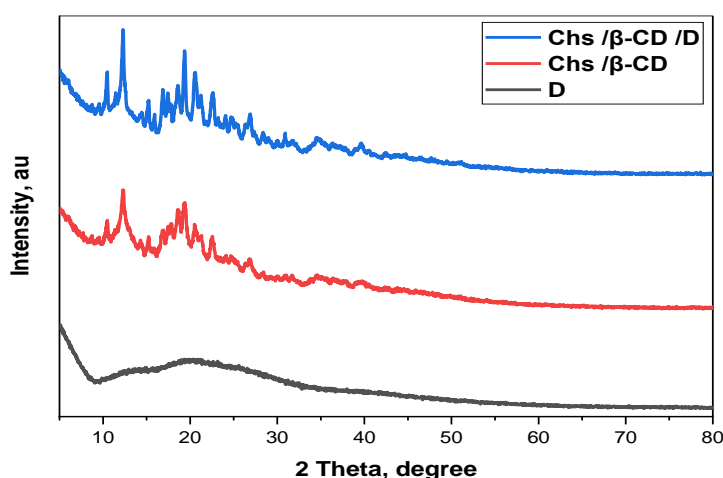


Figure 4. XRD spectra of D, Chs/ β -CD (1), Chs/ β -CD/D (3)b.

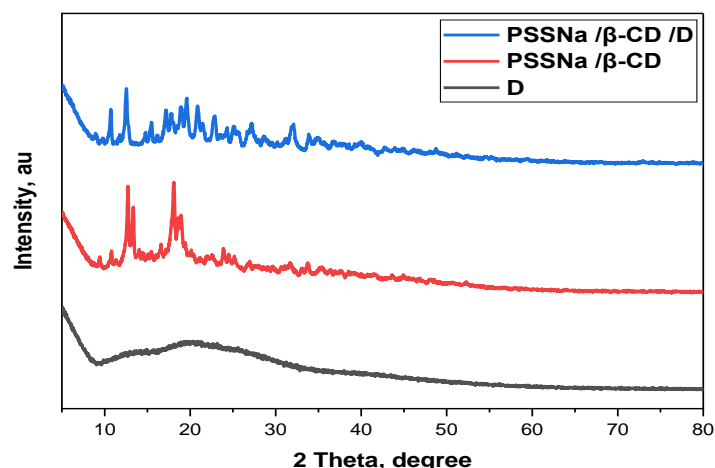


Figure 5. XRD spectra of D, PSSNa/β-CD (2), and PSSNa/β-CD/D (4).

Table 3. XRD peaks and crystallinity of D, Chs/β-CD (1) Chs/β-CD/D (3), PSSNa/β-CD (2) and PSSNa/β-CD/D (4).

Compound	2 Theta, degree	Intensity, au	Crystallinity
D	13.68	30.03	12.2%
	16.48	30.79	
	18.14	34.19	
	20.35	35.95	
	21.22	35.59	
Chs/β-CD (1)	10.43	59.95	74.7%
	12.27	80.54	
	18.58	68.33	
	19.37	72.62	
Chs/β-CD/D (3)	10.48	70.64	76.8%
	12.27	97.03	
	18.00	62.25	
	19.35	83.87	
PSSNa/β-CD (2)	10.48	70.64	51.6%
	12.27	97.03	
	18.00	62.25	
	19.35	83.87	
PSSNa/β-CD/D (4)	10.70	40.70	64.2%
	12.50	53.88	
	17.76	38.11	
	19.63	47.79	
	20.86	42.88	

3.4. Surface morphology.

The morphological structures of Streptomycin (D), Chs/β-CD (1), Chs/β-CD /D (3), PSSNa/β-CD (2), and PSSNa/β-CD/D (4) were indicated in Figure 6. The morphology structure of β-CD (A) and Streptomycin (B) is completely different from Chs/β-CD (C) and Chs/β-CD/D (E), which is referred to as the formation of pseudopolyrotaxane (1) and the effective loading of drug into the pseudopolyrotaxane (1). SEM image of Streptomycin (B) revealed amorphous, retractable, round-shaped particles. Furthermore, the SEM image of β-CD (A) appeared as a three-dimensional block structure with an irregular shape, while the SEM image of Chs/β-CD (C) appeared as homogeneous amorphous morphology, and Chs/β-CD/D (E) had an irregular block-like structure, and the original morphologies of the individual compounds disappeared. On the other hand, the morphological structure of pure Streptomycin (B) was changed after loading on PSSNa/β-CD (D). SEM image of PSSNa/β-CD (D) appeared

as needle-shaped crystals having various sizes, while the PSSNa/ β -CD/D (F) showed an irregular block-like structure.

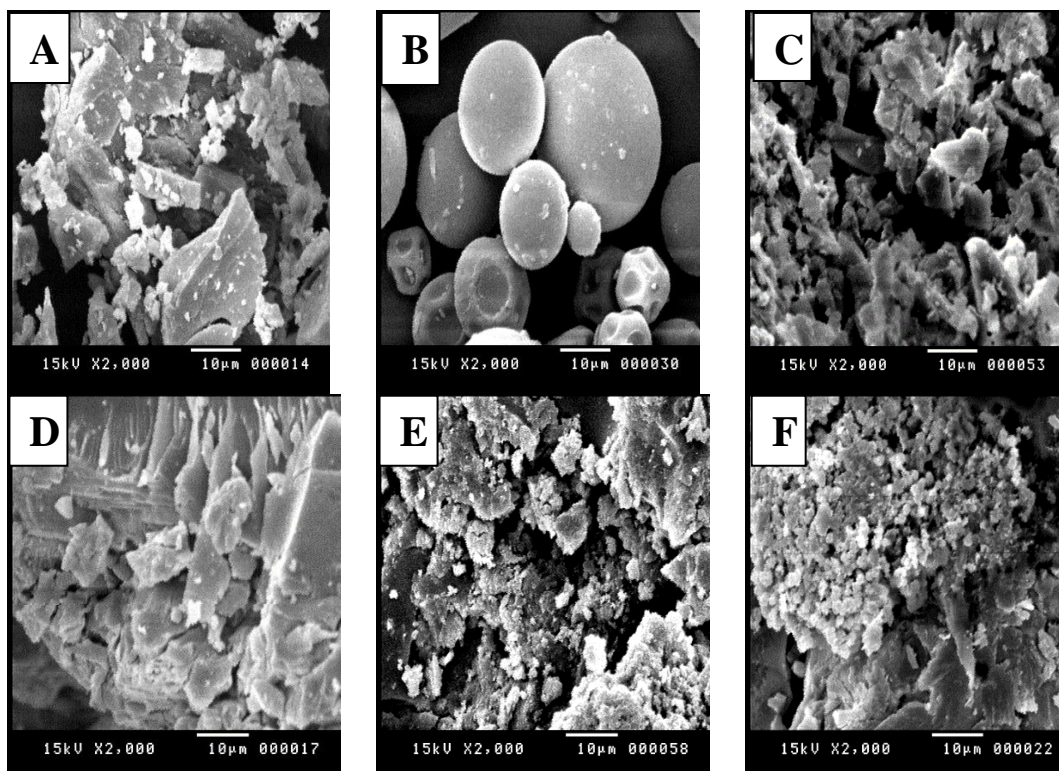


Figure 6. SEM images of (A) β -CD; (B) Streptomycin; (C) Chs/ β -CD; (D) PSSNa/ β -CD; (E) Chs/ β -CD/D; (F) PSSNa/ β -CD/D at magnification of 2000X.

3.5. Thermal analysis.

Figure 7 represents the thermal stability of Streptomycin D, Chs/ β -CD (1), Chs/ β -CD/D (3), PSSNa/ β -CD and PSSNa/ β -CD/D. Figure 7 indicates the change in the thermal stability of streptomycin D after loading on the prepared pseudopolyrotaxanes Chs/ β -CD (1) and PSSNa/ β -CD (2). Thus, there are three weight-loss stages (mg) versus temperature, up to 800°C under nitrogen, with the initial portion of the TGA curve up to 100°C due to moisture removal. From this figure, the loading of D on Chs/ β -CD (1) and PSSNa/ β -CD (2) improved the thermal stability of Streptomycin D up to 400°C. This property is very important for preventing the thermal degradation of the drug and is required during storage. Since Streptomycin is composed of a network of hydrogen bonds, electrostatic interactions prevent oxidation reactions and volatile species.

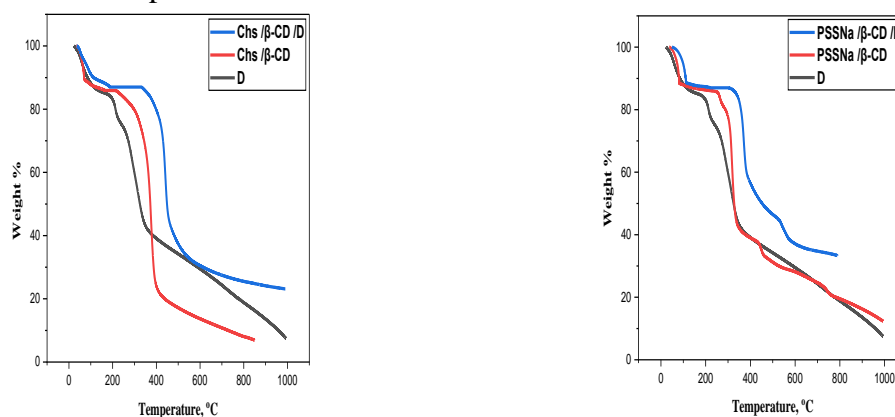


Figure 7. TGA curves of D, Chs/ β -CD (1) and Chs/ β -CD/D (3), PSSNa/ β -CD (2) and PSSNa/ β -CD/D (4).

3.6. Antibacterial performance evaluation.

3.6.1. Minimal inhibitory concentration (MIC).

The MIC values of the tested compounds Chs/ β -CD (1), PSSNa/ β -CD (2), Chs/ β -CD/D (3), and PSSNa/ β -CD/D (4) against *S. aureus* and *E. coli* ranged from 16 ~ 0.125 μ g/mL. The obtained values were compared with the MICs of Streptomycin, which was used as the standard drug. Most of the tested compounds demonstrated poor activity against *S. aureus*, except Chs/ β -CD/D, which greatly inhibited bacterial growth, with an MIC of 4 μ g/mL compared with Streptomycin (16 μ g/mL; Figures 8 and 9). On the other hand, the most effective compound against *E. coli* was Chs/ β -CD/D, which inhibited bacterial growth with an MIC of 4 μ g/mL, followed by PSSNa/ β -CD/D and Chs/ β -CD with MICs of 4 and 8 μ g/mL, respectively, compared to Streptomycin (16 μ g/mL). Also, no biological activity was recorded for β -CD and PSSNa/ β -CD against the same strain (Figure 10).

The results showed that the obtained PSSNa/ β -CD and Chs/ β -CD improved the solubility of the *S. aureus* and *E. coli* membranes and enhanced Streptomycin D penetration through them. In addition to, the drug after loading into the PSSNa/ β -CD and Chs/ β -CD was emerged with the surface of bacterial cell and causing damage in its external membrane and dispersion by the active transport, after that the drug was released from polymer carriers to link with protein cell via hydrogen bonds between the active groups in Streptomycin D (OH, NH, NH₂, CO) and active groups in proteins. These interactions lead to the killing of bacterial cells.

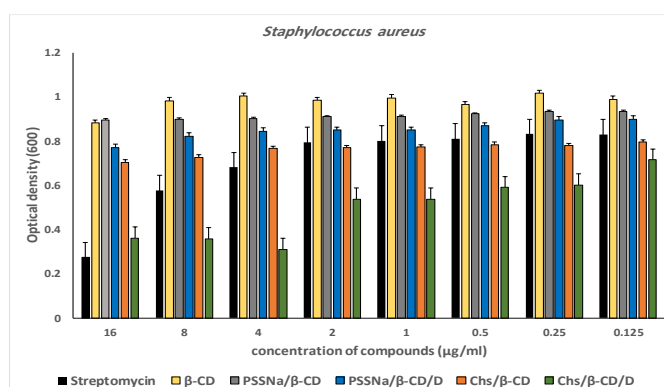


Figure 8. Antibacterial activities of Streptomycin, β -CD, PSSNa/ β -CD, PSSNa/ β -CD/D, Chs/ β -CD and Chs/ β -CD/D against *S. aureus*. OD600 represents bacterial growth. The graph displays the standard error of the mean of triplicate wells from one of three similar experiments.

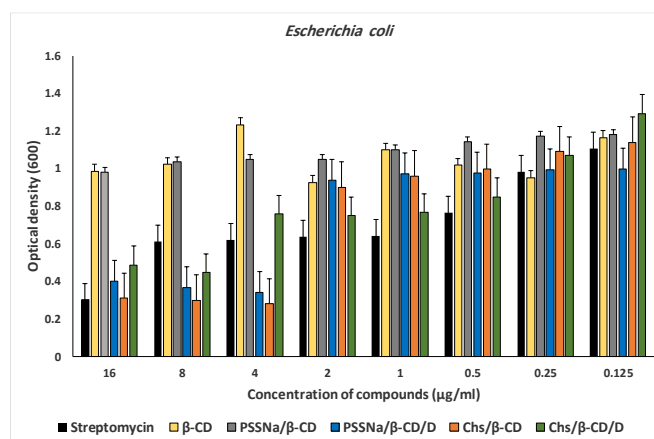


Figure 9. Antibacterial activities of Streptomycin, β -CD, PSSNa/ β -CD, PSSNa/ β -CD/D, Chs/ β -CD and Chs/ β -CD/D against *E. coli*. OD600 represents bacterial growth. The graph displays the standard error of the mean of triplicate wells from one of three similar experiments.

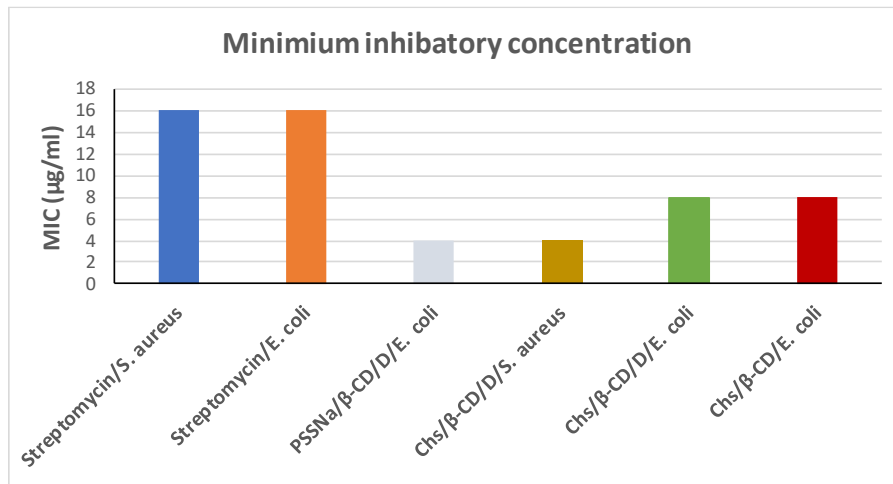


Figure 10. Minimum inhibitory concentration (MIC) of *Streptomycin/S. aureus*, *Streptomycin/E. coli*, PSSNa/ β -CD/D/*E. coli*, Chs/ β -CD/D/*S. aureus*, Chs/ β -CD/D/*E. coli*, and Chs/ β -CD/*E. coli*.

3.6.2. The effect of target compounds on biofilm formation.

Streptomycin loaded into a pseudopolyrotaxane; Chs/ β -CD can significantly inhibit biofilm formation by *S. aureus* and *E. coli* compared with Streptomycin alone. Pseudopolyrotaxane PSSNa/ β -CD with or without loaded Streptomycin had nearly similar effects to Streptomycin alone on the biofilm formation of *E. coli* Figure 11.

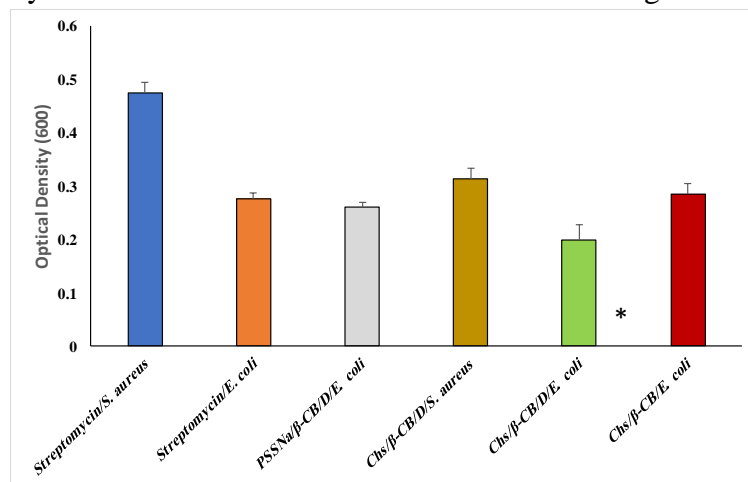


Figure 11. Effect of *Streptomycin* (PSSNa/ β -CD/D (4)), (Chs/ β -CD/D (3)) and (Chs/ β -CD (1)) on biofilm formation by *S. aureus* and *E. coli*. The graph displays the standard error of the mean of triplicate wells from one of three similar experiments. *versus *Streptomycin* $p < 0.05$.

Several studies demonstrated increased complexed drug bioactivity and concentration compared with free drug, due to better stability and protection from degradation [38]. The current results showed that Streptomycin, after loading onto pseudo-polyrotaxane (1) to form Chs/ β -CD/D (3), was more active against biofilm formation by *S. aureus* or *E. coli* than the free drug. Even β -CD complexed with chitosan without *Streptomycin* (Chs/ β -CD (1)) showed better antibacterial activity against *E. coli*. In contrast, the bioactivity of *Streptomycin*, when complexed with β -CD and PSSNa, against biofilm formation by *E. coli* showed that the complex is more active than the pristine drug.

4. Conclusion

Streptomycin is an antibiotic widely used to treat various bacterial infections. However, it has some adverse effects such as vertigo, vomiting, facial numbness, fever, and rash. For

these reasons, we aimed, in this study, to reduce these side effects by increasing the biological efficacy of Streptomycin, thereby minimizing the required drug dose for the desired treatment. This was accomplished via inserting biopolymer complexes (1) and (2); after that, *Streptomycin* was loaded into pseudopolyrotaxanes to afford the composites (3) and (4), thus improving the physicochemical properties and the efficiency of the drug. Significantly, the biological activity of the obtained composites has been greatly influenced by the loading of *Streptomycin* into pseudopolyrotaxanes (1) rather than pseudopolyrotaxanes (2), contrary to Gram-negative (*E. coli*) and Gram-positive (*S. aureus*) bacteria. The two types of products were also more active than the pure *Streptomycin* drug. Ultimately, activity is greater than the pure drug. This study focuses on improving the physical properties of Streptomycin, an antibiotic used to treat certain infectious diseases. In this study, the drug was improved by loading it on a new type of polymer containing cyclodextrin (polyrotaxanes). The biological efficiency of Streptomycin was proven after the loading process. This study can be applied to a wide range of drugs, especially those with high side effects (anti-cancer drugs), by improving their bioavailability and physical properties to increase their effectiveness and reduce their side effects. Generally, loading drugs into polymers is a promising strategy in drug delivery, offering several opportunities to enhance therapeutic outcomes, such as controlled and sustained release, targeted drug delivery, improved drug stability, and commercial and clinical potential.

Author Contributions

Conceptualization, K.D., H.D. and H.A.; methodology, H.D. M.E. and H.A.; software, H.D. M.E. and H.A.; validation, K.D., H.D., M. R., and A.N.; formal analysis, K.D., H.D. M. E., and H. A.; investigation, K.D., H.D. M. E., H. A. and M. R.; data curation, K.D., H.D. M. E., H. A. and M. R.; writing—original draft preparation, K.D., H.D. M. E., L. M., H. A., M. R., S. M., O, F., and A. N.; writing—review and editing, K.D., H.D. M. E., L. M., H. A., M. R., S. M., O, F., and A. N.; visualization, K.D., H.D. M. E., and H. A.; supervision, K.D., and H.D.; project administration, K.D., and H.D. All authors have read and agreed to the published version of the manuscript.

Institutional Review Board Statement

Not applicable.

Informed Consent Statement

Not applicable.

Data Availability Statement

Data supporting the findings of this study are available upon reasonable request from the corresponding author.

Conflicts of Interest

The authors declare no conflict of interest.

References

1. Mayur, A.C.; Senthilkumaran, K. Cyclodextrin In Drug Delivery: A Review. *Research and Reviews: Journal of Pharmacy and Pharmaceutical Sciences* **2012**, *1*, 19-29.
2. Dardeer, H.M.; Toghan, A.; Zaki, M.E.A.; Elamary, R.B. Design, Synthesis and Evaluation of Novel Antimicrobial Polymers Based on the Inclusion of Polyethylene Glycol/TiO₂ Nanocomposites in Cyclodextrin as Drug Carriers for Sulfaguanidine. *Polymers* **2022**, *14*, 227, <https://doi.org/10.3390/polym14020227>.
3. Jiang, B.; Guo, H.; Zhao, L.; Xu, B.; Wang, C.; Liu, C.; Fan, H. Fabrication of a β -cyclodextrin-based self-assembly containing a redox-responsive ferrocene *Soft Matter*. **2020**, *16*, 125-131, <https://doi.org/10.1039/C9SM02049G>.
4. Mehrarya, M.; Gharehchelou, B.; Kabarkouhi, Z.; Ataei, S.; Esfahani, F.N.; Wintirsiri, M.N.; Mozafari, M.R. Faunctionalized Nanostructured Bioactive Carriers: Nanoliposomes, Quantum Dots, Tocosome, and Theranostic Approach. *Current Drug Delivery* **2022**, *19*, 1001-1011, <http://dx.doi.org/10.2174/1567201819666220324092933>.
5. Li, Z.; Liu, H.; Qi, C.; Yang, A.; Deng, S. Preparation, characterization and molecular modelling of inclusion complex between α -naphthylacetic acid with ethylenediamine- β -cyclodextrin. *J Incl Phenom Macrocycl Chem* **2019**, *93*, 289-299, <https://doi.org/10.1007/s10847-018-00875-6>.
6. Ibrahim, A.S.; Gad, A.N.; Dardeer, H.M.; Gaber, A.M. Chitosan-Cellulose Nanocomposite: Preparation, characterization, and evaluation as cationic color precipitant in sugar clarification process. *Food Chemistry* **2023**, *415*, 135603, <https://doi.org/10.1016/j.foodchem.2023.135603>.
7. Liu, Y.; Lin, T.; Cheng, C.; Wang, Q.; Lin, S.; Liu, C.; Han, X. Research progress on synthesis and application of cyclodextrin polymers. *Molecules* **2021**, *26*, 1090.
8. Lou, C.; Tian, X.; Deng, H.; Wang, Y.; Jiang, X. Dialdehyde- β -cyclodextrin-crosslinked carboxymethyl chitosan hydrogel for drug release. *Carbohydr. Polym.* **2020**, *231*, 115678.
9. Machín, R.; Isasi, J.R.; Vélaz, I. β -Cyclodextrin hydrogels as potential drug delivery systems. *Carbohydrate Polymers* **2012**, *87*, 2024-2030, <https://doi.org/10.1016/j.carbpol.2011.10.024>.
10. Dardeer, H.M.; Ibrahim, A.S.; Gad, A.N.; Gaber, A.A.M. Bifunctional of Fe₃O₄@ chitosan nanocomposite as a clarifying agent and cationic flocculant on different sugar solutions as a comprehensive semi industrial application. *Scientific Reports* **2024**, *14*, 1848, <https://doi.org/10.1038/s41598-024-52111-6>.
11. Takahashi, K.; Hayashita, T. Special issue "cyclodextrins: past, present, and future. *J. Inclus. Phenomena Macrocycl. Chem.* **2019**, *93*, 1, <https://doi.org/10.1007/s10847-018-0860-7>.
12. Srivastava, A.; Yadav, T.; Sharma, S.; Nayak, A.; Kumari, A.; Mishra, N. Polymers in Drug Delivery. *J. Biosci. Med.* **2016**, *4*, 69-84, <http://dx.doi.org/10.4236/jbm.2016.41009>.
13. Yanat, M.; Schroën, K. Preparation methods and applications of chitosan nanoparticles; with an outlook toward reinforcement of biodegradable packaging. *React. Funct. Polym.* **2021**, *161*, 104849, <https://doi.org/10.1016/j.reactfunctpolym.2021.104849>.
14. Kedir, W.M.; Abdi, G.F.; Goro, M.G.; Tolesa, L.D. Pharmaceutical and drug delivery applications of chitosan biopolymer and its modified nanocomposite: A review. *Heliyon* **2022**, *8*, e10196, <https://doi.org/10.1016/j.heliyon.2022.e10196>.
15. Vinjamuri, B.P.; Kotha, A.K.; Kolte, A.; Haware, R.V.; Chougule, M.B. Chapter 12 - Polymer Applications in Pulmonary Drug Delivery. In *Applications of Polymers in Drug Delivery (Second Edition)*, Misra, A., Shahiwala, A., Eds.; Elsevier: **2021**; pp. 333-354, <http://dx.doi.org/10.1016/B978-0-12-819659-5.00012-4>.
16. Alazmi, A.A.; Dawood, K.M.; Al-Matar, H.M.; Tohamy, W.M. Clean and Efficient Green Protocol of *N,N'*-Bis(2-(aryloxy)-2-(aryloxy)vinyl)ethane-1,2-diamines in Aqueous Medium without Catalyst: Synthesis and Photophysical Characterization. *ACS Omega* **2022**, *7*, 28831-28848, <https://doi.org/10.1021/acsomega.4c06250>.
17. Rashdan, H.R.M.; El-Sayyad, G.S.; Shehadi, I.S.; Abdelmonsef, A.H. Antimicrobial potency and *E. coli* β -carbonic anhydrase inhibition efficacy of phenazone-based molecules. *Molecules* **2023**, *28*, 7491, <https://doi.org/10.3390/molecules28227491>.
18. Subhash, N.E.; Nair, S.; Srinivas, S.P.; Theruveethi, N.; Bhandary, S.V.; Guru, B.R. Development of a biodegradable polymer-based implant to release dual drugs for post-operative management of cataract surgery. *Drug Deliv. Transl. Res* **2024**, *15*, 508-522, <https://doi.org/10.1007/s13346-024-01604-y>.

19. Nadia, A.A.; Hrichi, E.H.; Alolayan, R.A.; Derafa, W.; Zahou, F.M.; Bakr, R.B. Synthesis of Chalcones Derivatives and Their Biological Activities: A Review. *ACS Omega* **2022**, *7*, 27769-27786, <https://doi.org/10.1021/acsomega.2c01779>.
20. Dardeer, H.M.; Taha, A.G.; Toghan, A.; Abdelmonsef, A.H. Synthesis, In silico Molecular Docking Studies and antimicrobial evaluation of Some New Anthracene Derivatives Tagged with Arylidene, Pyridine, Oxazole, and Chromene Moieties as Promising Inhibitors of Bacterial DNA gyrase. *Biointerface Res. Appl. Chem.* **2023**, *13*, 299, <https://doi.org/10.33263/BRIAC133.299>.
21. Xu, C.; Wang, Y.; Guo, Z.; Chen, J.; Lin, L.; Wu, J.; Chen, X.J. Pulmonary delivery by exploiting doxorubicin and cisplatin co-loaded nanoparticles for metastatic lung cancer therapy. *Control. Release* **2019**, *295*, 153-163, <https://doi.org/10.1016/j.jconrel.2018.12.013>.
22. Dardeer, H.M.; Abbas, S.A.; El-Sayyad, G.S.; Ali, M.F. Effect of titanium dioxide nanoparticles and β -cyclodextrin polymer on physicochemical, antimicrobial, and antibiofilm properties of a novel chitosan-camphor polymer. *Internat. J. Biol. Macromol.* **2022**, *219*, 1062-1079, <https://doi.org/10.1016/j.ijbiomac.2022.07.249>.
23. Zielińska, A.; Carreiró, F.; Oliveira, A.M.; Neves, A.; Pires, B.; Venkatesh, D.N.; Durazzo, A.; Lucarini, M.; Eder, P.; Silva, A.M.; et al. Polymeric Nanoparticles: Production, Characterization, Toxicology and Ecotoxicology. *Molecules* **2020**, *25*, 3731, <https://doi.org/10.3390/molecules25163731>.
24. Wenz, G.; Han, B.-H.; Müller, A. Cyclodextrin rotaxanes and polyrotaxanes. *Chem. Rev* **2006**, *106*, 782-817, <https://doi.org/10.1021/cr970027+>.
25. Harada, A. Cyclodextrin-based molecular machines. *Acc. Chem. Res.* **2001**, *34*, 456-464, <https://doi.org/10.1021/ar000174l>.
26. Dardeer, H.M.; Taha, A.G.; Abouzeid, R.E.; Aly, M.F. Novel chitosan-acetyl isatin polymer derivatives: synthesis, characterization, and applications in bone tissue engineering. *Biomass Convers. Biorefin.* **2022**, *14*, 12427-12440, <https://doi.org/10.1007/s13399-022-03176-8>.
27. Chakraborty, G.; Ray, A.K.; Singh, P.K.; Pal, H. Does the degree of substitution on the cyclodextrin hosts impact their affinity towards guest binding?. *Photochem. Photobiol. Sci* **2020**, *19*, 956-965, <https://doi.org/10.1039/d0pp00103a>.
28. Radwan, M.F.; Dardeer, H.M.; Elboray, E.E.; Aly, M.F. Novel crystalline and thermally stable chitosan-chromone based polymers: Synthesis and characterization. *J. Mol. Struct.* **2021**, *1241*, 130625, <https://doi.org/10.1016/j.molstruc.2021.130625>.
29. Dzedzic, I; Kertmen, A. Methods of chitosan identification: History and Trends. *Lett. Appl. NanoBioSci.* **2023**, *12*, 94, <http://doi.org/10.33263/LIANBS124.094>.
30. Dawood, K.M.; Dardeer, H.M.; Abdel atty, H.A.; El. Hassan, M.; Rasslan, M.A.; Mohamed, S.K.; Farghaly, O.A.; Nafady, A. Design, assessment and antibacterial potency of novel pseudopoly-rotaxanes based on cyclodextrin as drug carriers for amoxicillin and ceftriaxone. *J. Mol. Struct.* **2024**, *1296*, 136906, <https://doi.org/10.1016/j.molstruc.2023.136906>.
31. Junejo, J.A.; Zaman, K.; Rudrapal, M. Hepatoprotective and Anti-inflammatory Activities of Hydro-alcoholic Extract of Oxalis debilis Kunth.Leaves. *Lett. Appl. NanoBioScience* **2022**, *11*, 3626-3633, <http://doi.org/10.33263/LIANBS113.36263633>.
32. Low, D. Reducing antibiotic use in influenza: Challenges and rewards. *Clin. Microbiol. Infect.* **2008**, *14*, 298-306.
33. Yousef, N.M. Antimicrobial agents produced by Streptomycin. In Understanding microbial pathogens: current knowledge and educational ideas on antimicrobial research. Torres-Hergueta, E., Méndez-Vilas, A., Eds.; **2018**.
34. Mondal, M.K.; Mukherjee, S.; Joardar, N.; Roy, D.; Chowdhury, P.; Babu, S.P.S. Synthesis of smart graphene quantum dots: A benign biomaterial for prominent intracellular imaging and improvement of drug efficacy. *Appl. Surface Sci* **2019**, *495*, 143562, <https://doi.org/10.1016/j.apsusc.2019.143562>.
35. Singh, A.; Gautam, P.K.; Verma, A.; Singh, V.; Shivapriya, P.M.; Shivalkar, S.; Samanta, S.K. Green synthesis of metallic nanoparticles as effective alternatives to treat antibiotics resistant bacterial infections: A review. *Biotechnol. Reports* **2020**, *25*, e00427, <https://doi.org/10.1016/j.btre.2020.e00427>.
36. Bhattacharya, D.; Samanta, S.; Mukherjee, A.; Santra, C. R.; Ghosh, A. N.; Niyogi, S. K.; Karmakar, P. J. Antibacterial Activities of Polyethylene Glycol, Tween 80 and Sodium Dodecyl Sulphate Coated Silver Nanoparticles in Normal and Multi-Drug Resistant Bacteria. *Nanosci. Nanotechnol.* **2012**, *12*, 2513-2521, <https://doi.org/10.1166/jnn.2012.6148>.

37. Chowdhury, S.K.; Dutta, T.; Chattopadhyay, A.P.; Ghosh, N.N.; Chowdhury, S.; Manda, V. Isolation of antimicrobial Tridecanoic acid from *Bacillus* sp. LBF-01 and its potentialization through silver nanoparticles synthesis: a combined experimental and theoretical studies. *J. Nanostructure Chem* **2021**, *11*, 573–587, <https://doi.org/10.1007/s40097-020-00385-3>.
38. Dutta, T.; Chowdhury, S.K.; Ghosh, N.N.; Chattopadhyay, P.A.; Das, M.; Manda, V. Green synthesis of antimicrobial silver nanoparticles using fruit extract of *Glycosmis pentaphylla* and its theoretical explanations. *J. Mol. Struct.* **2022**, *1247*, 131361, <https://doi.org/10.1016/j.molstruc.2021.131361>.

Publisher's Note & Disclaimer

The statements, opinions, and data presented in this publication are solely those of the individual author(s) and contributor(s) and do not necessarily reflect the views of the publisher and/or the editor(s). The publisher and/or the editor(s) disclaim any responsibility for the accuracy, completeness, or reliability of the content. Neither the publisher nor the editor(s) assume any legal liability for any errors, omissions, or consequences arising from the use of the information presented in this publication. Furthermore, the publisher and/or the editor(s) disclaim any liability for any injury, damage, or loss to persons or property that may result from the use of any ideas, methods, instructions, or products mentioned in the content. Readers are encouraged to independently verify any information before relying on it, and the publisher assumes no responsibility for any consequences arising from the use of materials contained in this publication.